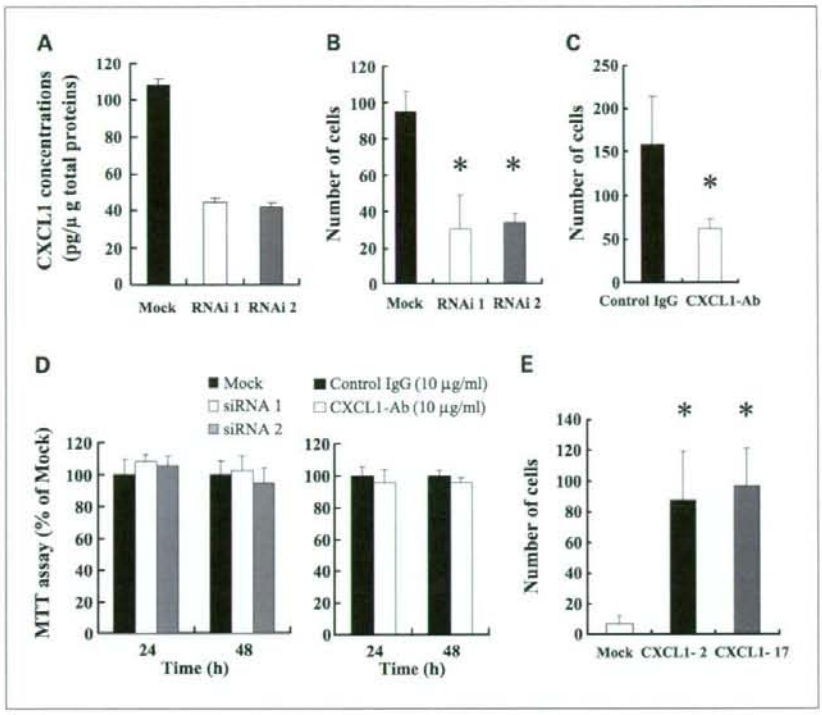

Fig. 3. *A*, knockdown of CXCL1 by RNAi vector in T24 cells was confirmed by ELISA. Values were corrected for the total protein in the cell lysate. Bars, SD. *B*, invasive potential of CXCL1 knockdown clones. After 8 h, the cells on the lower surface of the filter were counted. *, $P < 0.01$, compared with mock clones. *C*, effect of neutralizing antibody to CXCL1 on invasive ability. T24 cells were incubated in RPMI 1640 with 10% FCS containing 10 μg/mL anti-CXCL1 or control IgG for 48 h. Then, the cells were subsequently placed in the upper compartment of an invasion chamber in serum-free RPMI 1640 containing 10 μg/mL anti-CXCL1 or control IgG and incubated at 37°C under 5% CO_2. After 8 h, the cells on the lower surface of the filter were counted. *, $P < 0.05$, compared with control IgG. *D*, effect of CXCL1 knockdown and neutralizing antibody to CXCL1 on proliferation rate of T24 cells. The cell proliferation was determined by the 3-(4,5-dimethylthiazol-2-yl)-2,5-diphenyltetrazolium bromide (*MTT*) assay. No significant difference was detected. *E*, CXCL1 overexpression increased the invasiveness of RT112 cells. After 60 h of incubation, cells on the lower surface of the filter were counted. *, $P < 0.01$, compared with mock clones. Columns, each result of a modified Boyden chamber assay is expressed as the mean of the number of cells in the five densest spots identified on the lower surface of the filter within a single ×200 field in each of three experiments; bars, SD. A representative experiment is shown.

The level of CXCL1 in the urine reflects the existence of bladder cancer. Because immunohistochemical analysis showed that bladder tumors express CXCL1 *in vivo*, we determined if an increase of CXCL1 in the urine could indicate the existence of bladder cancer, especially that with invasive phenotype. The amount of CXCL1 in the urine was examined in 67 patients with histopathologically proven bladder cancer and 31 controls. Because it was shown that several chemokines are elevated in patients with febrile urinary tract infections (28), we eliminated urine samples contaminated with >30 leukocytes per microscopic field. The concentration of CXCL1 in the urine was examined by ELISA and corrected by the urinary creatinine level (Fig. 5A). The mean corrected CXCL1 level in the control group and in patients with noninvasive and invasive tumors was 7.8 ± 2.5, 17 ± 3.7, and 112 ± 25 pg/mg creatinine (mean ± SE), respectively. It was revealed that the corrected CXCL1 level from both noninvasive pTa tumors and invasive pT1-4 tumors was significantly higher than those in the controls ($P = 0.0076$ and $P < 0.0001$, respectively). More importantly, a significant difference was observed between noninvasive and invasive tumors ($P = 0.0028$). These results suggested that the corrected CXCL1 level in the urine would predict the existence of both noninvasive and invasive bladder tumors. So, we have done the ROC curve analysis to estimate the optimal cutoff point. Using 9.5 pg/mg creatinine as the cutoff value to predict the existence of noninvasive or invasive bladder cancer, measurement of the corrected urine CXCL1 level had a sensitivity of 70.1% and a specificity of 80.6% (area under the curve, 0.782; Fig. 5B). Furthermore, using 37.5 pg/mg creatinine as the cutoff value to predict particularly invasive bladder cancer, measurement of corrected CXCL1 had a sensitivity of 57.1% and a specificity of 90.6% (area under the curve, 0.713; Fig. 5C). Finally, we have done multivariate stepwise logistic regression analysis incorporating CXCL1 as a continuous variable, cytology, age, and sex to examine that the corrected CXCL1 level could be an independent factor for predicting the invasive bladder cancer. It was revealed that cytology (odds ratio, 21.82; 95% confidence interval, 3.981-113.780; $P = 0.003$) and CXCL1 (odds ratio, 1.023; 95% confidence interval, 1.001-1.044; $P = 0.038$) were independent factors for predicting the bladder cancer with invasive phenotype (Table 1).

Discussion

Tumor cells overexpress many secreted proteins; some of these can be detected in serum samples from patients with cancer and have been considered as potential new tumor markers (29). Well-known secreted proteins that are used as biomarkers include α-fetoprotein for liver cancer or nonseminomatous germ cell tumors, as well as prostate-specific antigen for prostate cancer (30). Our previous analysis of serum-free cell culture supernatants showed that proteins in the culture supernatant reflected those produced by tumor cells *in vivo* (11). This observation strongly suggests that systematic analysis of the proteins secreted by cultured cancer cells will contribute to the identification of potential diagnostic and prognostic tumor biomarkers.

We compared the protein profile between highly invasive (T24) and less invasive (RT112) bladder cancer cell lines.

Candidate proteins were further screened using the cellular localization information from the Swiss-Prot database. Consequently, CXCL1 was significantly higher in invasive tumors than in noninvasive tumors *in vivo* (Fig. 2A).

CXCL1 is a member of the CXC chemokine family (31). This family of molecules can be classified according to the presence or absence of three amino acid residues (Glu-Leu-Arg; ELR motif) that precede the first cysteine amino acid residue in the primary structure (32). The ELR$^+$ CXC chemokines (CXCL1, CXCL2, CXCL3, CXCL5, CXCL6, CXCL7, and CXCL8) are chemoattractants for neutrophils and are also potent angiogenic factors (33–35). In contrast, ELR$^-$ CXC chemokines (CXCL4, CXCL9, and CXCL10) are chemoattractants for mononuclear cells and are potent inhibitors of angiogenesis (35, 36). In a variety of human cancers, the ELR$^+$ CXC chemokines have been found to be associated with tumorigenesis, angiogenesis, and metastasis (25, 37). The biological functions of ELR$^+$ CXC chemokines are primarily mediated via CXCR2, a seven-transmembrane G protein–coupled receptor. CXCL1 protein was originally purified from the culture supernatant of Hs29T melanoma cells and is also known as melanoma growth stimulatory activity α or growth-related protein α (38, 39). Although the elevated expression of CXCL1 has been reported in a series of human tumors (40, 41), the role of this chemokine in bladder cancer is poorly understood. In this study, we showed that higher expression of CXCL1 was associated with the invasive phenotype of bladder cancer both *in vitro* and *in vivo* (Fig. 2). We also showed that the secreted CXCL1 was sufficient for the invasion of bladder tumors *in vitro* (Fig. 3). Because the CXCL1 receptor CXCR2 is expressed in all the bladder cancer cell lines (Fig. 2B) and in most of the tumor tissues examined irrespective of the invasion phenotype (microarray analysis; data not shown), it is probable that secreted CXCL1 is associated with the invasion of the bladder cancer via an autocrine loop involving its receptor.

CXCL1 did not induce bladder cancer cell proliferation, although it has been shown to promote cell proliferation in several types of tumors. Its interaction with CXCR2 is shown to induce extracellular signal-regulated kinase 1/2 phosphorylation, which then leads to induction of EGR1, and these are responsible for increased cell proliferation (37). Therefore, we examined the extracellular signal-regulated kinase 1/2 pathway in T24 and RT112 cells in which CXCL1 was engineered to be repressed or overexpressed, respectively. It was revealed that CXCL1 did not induce this pathway in bladder cancer cells (data not shown).

As for the mechanisms by which CXCL1 regulates the invasive ability of bladder cancer cells, we found for the first time that this chemokine induced MMP-13 *in vitro* (Fig. 4A). Although it is still uncertain if this is also true *in vivo*, a recent study showed that MMP-13 is highly expressed in invasive bladder tumor tissue (24), supporting our preliminary immunostaining results (Fig. 4B). As for other MMPs, Zhou et al. (42) reported that a glioma cell line overexpressing CXCL1 showed an increase in motility and invasiveness and that CXCL1-transfected cells showed increased expression of MMP-2. However, the expression of MMP-2 was not affected by the introduction of CXCL1 in RT112 cell lines (data not shown). CXCL1 may regulate the invasion of tumors through several types of MMPs. It has also been reported that this chemokine regulates the expression of several proteins, such as β_3 integrin, SPARC (42), vascular endothelial growth factor, and angiopoietin-2 (43). So, several factors including MMP-13 are likely to be involved in CXCL1-mediated regulation of bladder cancer invasion.

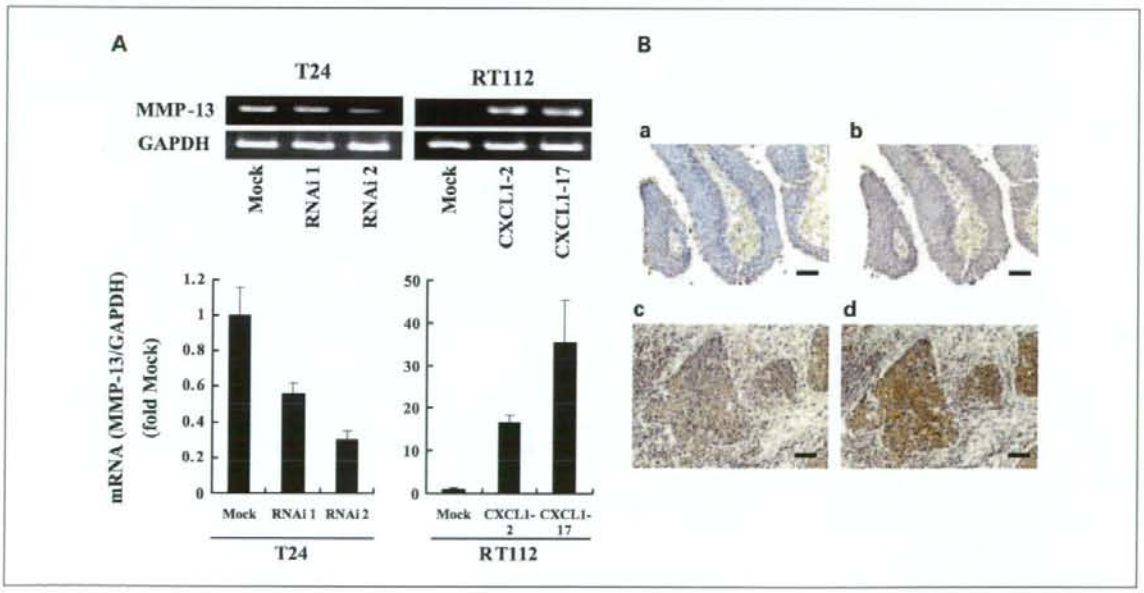

Fig. 4. *A*, expression of MMP-13 mRNA in T24 and RT112 cells in which CXCL1 was engineered to be repressed or overexpressed. RNAi knockdown of CXCL1 in T24 cells resulted in a decreased expression of MMP-13 and RT112 cells engineered to produce CXCL1 acquired the highly increased expression of MMP-13. Top, RT-PCR; bottom, real-time quantitative PCR. Bars, SD. *B*, immunohistochemical staining for CXCL1 and MMP-13 in bladder cancer tissues. Representative samples are shown. *a* and *c*, CXCL1; *b* and *d*, MMP-13. *a* and *b*, pT3G2 tumors showing diffuse cytoplasmic immunoreactivity; *c* and *d*, pTaG1 tumor without specific immunosignal. Bars, 100 μm.

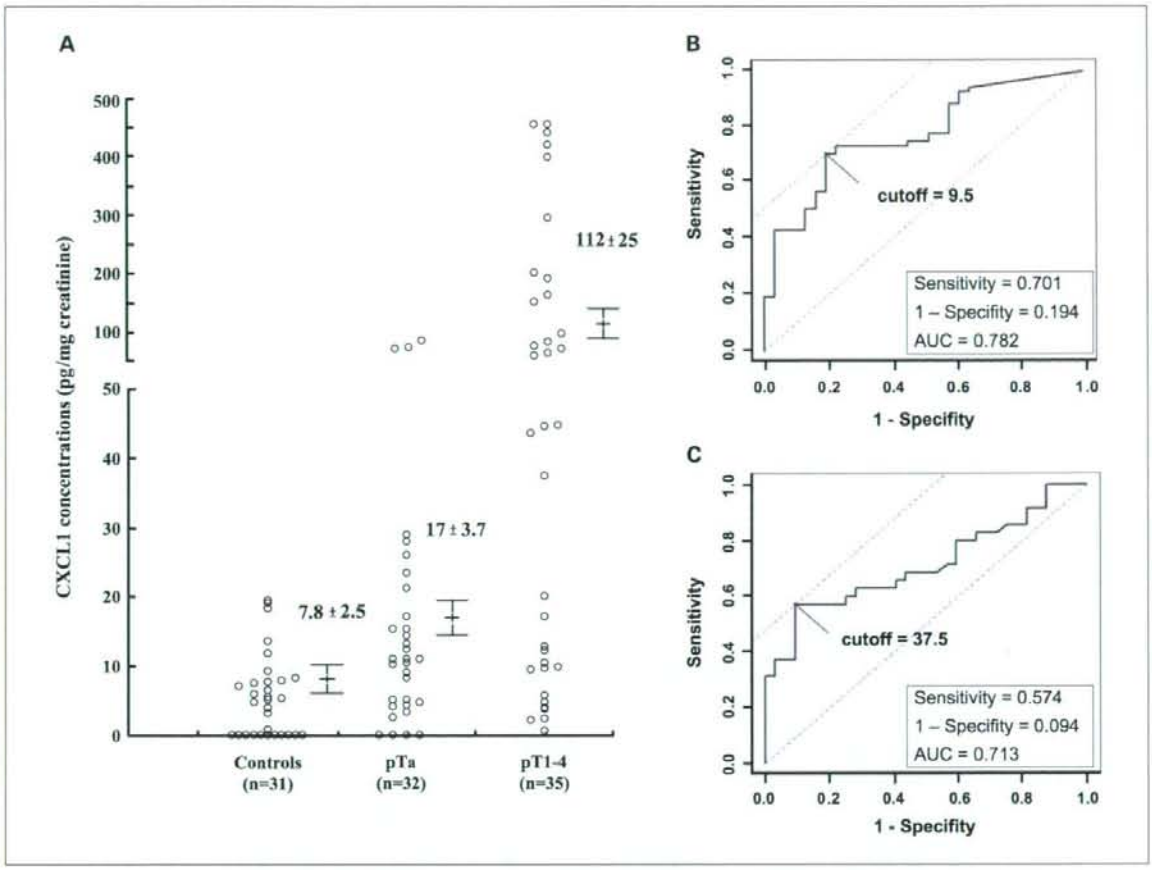

Fig. 5. *A*, CXCL1 levels in the urine of controls and patients with bladder cancer. Values were corrected by the urine creatinine concentration. Points, mean; bars, SE. *B*, ROC curve analysis of the urinary CXCL1 levels. The optimal cutoff of the urinary CXCL1 levels for distinguishing bladder tumor from control was determined as 9.5 using the ROC curve. *C*, ROC curve analysis of the urinary CXCL1 levels for distinguishing invasive from noninvasive bladder tumor. For all patients with bladder tumor, the optimal cutoff value of the urinary CXCL1 levels for distinguishing invasive from noninvasive bladder tumor was determined as 37.5 using ROC curve analysis.

Many studies have focused on the detection of specific bladder cancer–associated proteins in the urine of patients. Thus far, BTA, BTA stat, NMP22, and fibrinogen degradation products have been used as commercial diagnostic markers for bladder cancer in the urine (44). In addition, a lot of soluble urine marker is reported (45, 46). However, none of these markers is sensitive enough for routine clinical use (44). Recently, several investigators have proposed that high-throughput technologies, such as gene expression microarrays or proteomics, may be a new way to identify biomarkers for urothelial cancer in the urine (7, 47), and it is expected that this technology will be more widely used to identify novel cancer biomarkers in the future. In the present study, we showed for the first time that the level of CXCL1 was elevated in the urine from patients with bladder cancer (Fig. 5). These results indicate that an elevated CXCL1 in the urine could predict the existence of bladder cancer, especially in patients with invasive disease. Our results suggest that measurement of the level of CXCL1 in urine may be a useful biomarker for the early detection of invasive bladder cancer, and the inhibition of signals through CXCL1 might be a potent therapeutic target for preventing the progression of the bladder cancer. Additionally, CXCL8, one of ELR CXC chemokines that share 44% amino acid sequence identity with CXCL1 and are reported to be elevated in the urine of patients with transitional cell carcinoma (48). Further prospective and comparative studies in a different population are required for the precise evaluation of diagnostic values of CXC chemokines in bladder cancer.

Table 1. Multivariable stepwise logistic regression analyses of CXCL1, cytology, age, and sex for prediction of invasive stage (≥T1)

Variable	Odds ratio (95% confidence interval)	*P*
CXCL1*	1.023 (1.001-1.044)	0.038
Cytology (positive vs negative)	21.82 (3.981-113.7)	0.003

*Urinary CXCL1 levels were analyzed as continuous variables.

The role of chronic inflammation in cancer progression continues to gain importance in the biological events for several types of cancers. Recurrent or persistent inflammation may induce, promote, or influence susceptibility to carcinogenesis by causing DNA damage, inciting tissue reparative proliferation, and/or creating a stromal "soil" that is enriched with cytokines and growth factors (49). The evidence for an association between chronic inflammation and squamous cell carcinoma of the bladder is strong and widely accepted. In transitional cell carcinoma of the bladder, several animal and human studies strongly support the hypothesis that chronic inflammation induced by persistent urinary tract infections plays a role in the bladder carcinogenesis (50). As CXC chemokines, including CXCL1, play major roles in inflammation and wound healing (25). So, further understanding of roles of these chemokines on the tumorigenesis and disease progression of bladder cancer will be required to provide a new rationale for targeted therapy for this tumor.

Acknowledgments

We thank all members of Urine test room, Department of Clinical Laboratory, Kyoto University Hospital, for analyzing urine samples and Tomoko Matsushita and Chie Hagihara for their valuable technical assistance.

References

1. Borden LS, Jr., Clark PE, Hall MC. Bladder cancer. Curr Opin Oncol 2003;15:227–33.
2. Jemal A, Siegel R, Ward E, et al. Cancer statistics, 2006. CA Cancer J Clin 2006;56:106–30.
3. Lapham RL, Ro JY, Staerkel GA, Ayala AG. Pathology of transitional cell carcinoma of the bladder and its clinical implications. Semin Surg Oncol 1997;13:307–18.
4. Juffs HG, Moore MJ, Tannock IF. The role of systemic chemotherapy in the management of muscle-invasive bladder cancer. Lancet Oncol 2002;3:738–47.
5. Knowles MA. Molecular subtypes of bladder cancer: Jekyll and Hyde or chalk and cheese? Carcinogenesis 2006;27:361–73.
6. Hafner C, Knuechel R, Zanardo L, et al. Evidence for oligoclonality and tumor spread by intraluminal seeding in multifocal urothelial carcinomas of the upper and lower urinary tract. Oncogene 2001;20:4910–5.
7. Sanchez-Carbayo M. Use of high-throughput DNA microarrays to identify biomarkers for bladder cancer. Clin Chem 2003;49:23–31.
8. Zwickl H, Traxler E, Staettner S, et al. A novel technique to specifically analyze the secretome of cells and tissues. Electrophoresis 2005;26:2779–85.
9. Welsh JB, Sapinoso LM, Kern SG, et al. Large-scale delineation of secreted protein biomarkers overexpressed in cancer tissue and serum. Proc Natl Acad Sci U S A 2003;100:3410–5.
10. Diamandis EP. How are we going to discover new cancer biomarkers? A proteomic approach for bladder cancer. Clin Chem 2004;50:793–5.
11. Nakamura E, Abreu-e-Lima P, Awakura Y, et al. Clusterin is a secreted marker for a hypoxia-inducible factor-independent function of the von Hippel-Lindau tumor suppressor protein. Am J Pathol 2006;168:574–84.
12. Lee S, Nakamura E, Yang H, et al. Neuronal apoptosis linked to EglN3 prolyl hydroxylase and familial pheochromocytoma genes: developmental culling and cancer. Cancer Cell 2005;8:155–67.
13. Rabilloud T. Two-dimensional gel electrophoresis in proteomics: old, old fashioned, but it still climbs up the mountains. Proteomics 2002;2:3–10.
14. He P, He HZ, Dai J, et al. The human plasma proteome: analysis of Chinese serum using shotgun strategy. Proteomics 2005;5:3442–53.
15. Wolters DA, Washburn MP, Yates JR III. An automated multidimensional protein identification technology for shotgun proteomics. Anal Chem 2001;73:5683–90.
16. Williams SV, Sibley KD, Davies AM, et al. Molecular genetic analysis of chromosome 9 candidate tumor-suppressor loci in bladder cancer cell lines. Genes Chromosomes Cancer 2002;34:86–96.
17. Tazaki H, Tachibana M. Studies on KU-1 and KU-7 cells as an *in vitro* model of human transitional cell carcinoma of urinary bladder. Hum Cell 1988;1:78–83.
18. Masters JR, Hepburn PJ, Walker L, et al. Tissue culture model of transitional cell carcinoma: characterization of twenty-two human urothelial cell lines. Cancer Res 1986;46:3630–6.
19. Grossman HB, Wedemeyer G, Ren L, Wilson GN, Cox B. Improved growth of human urothelial carcinoma cell cultures. J Urol 1986;136:953–9.
20. Pfluger KH, Probeck HD, Adler G, Stach-Machado D, Kapmeyer H, Havemann K. Karyotype and ultrastructure of a colony stimulating factor (CSF) producing cell line (5637) originated from a carcinoma of the human urinary bladder. Blut 1986;53:89–100.
21. Williams RD. Human urologic cancer cell lines. Invest Urol 1980;17:359–63.
22. Tanaka Y, Akiyama H, Kuroda T, et al. A novel approach and protocol for discovering extremely low-abundance proteins in serum. Proteomics 2006;6:4845–55.
23. Matsui S, Ito M, Nishiyama H, et al. Genomic characterization of multiple clinical phenotypes of cancer using multivariate linear regression models. Bioinformatics 2007;23:732–8.
24. Bostrom PJ, Ravanti L, Reunanen N, et al. Expression of collagenase-3 (matrix metalloproteinase-13) in transitional-cell carcinoma of the urinary bladder. Int J Cancer 2000;88:417–23.
25. Tanaka T, Bai Z, Srinoulprasert Y, Yang BG, Hayasaka H, Miyasaka M. Chemokines in tumor progression and metastasis. Cancer Sci 2005;96:317–22.
26. Li A, Varney ML, Singh RK. Constitutive expression of growth regulated oncogene (gro) in human colon carcinoma cells with different metastatic potential and its role in regulating their metastatic phenotype. Clin Exp Metastasis 2004;21:571–9.
27. Takamori H, Oades ZG, Hoch OC, Burger M, Schraufstatter IU. Autocrine growth effect of IL-8 and GROα on a human pancreatic cancer cell line, Capan-1. Pancreas 2000;21:52–6.
28. Otto G, Burdick M, Strieter R, Godaly G. Chemokine response to febrile urinary tract infection. Kidney Int 2005;68:62–70.
29. Wu CC, Chien KY, Tsang NM, et al. Cancer cell-secreted proteomes as a basis for searching potential tumor markers: nasopharyngeal carcinoma as a model. Proteomics 2005;5:3173–82.
30. Balk SP, Ko YJ, Bubley GJ. Biology of prostate-specific antigen. J Clin Oncol 2003;21:383–91.
31. Wang D, Yang W, Du J, et al. MGSA/GRO-mediated melanocyte transformation involves induction of Ras expression. Oncogene 2000;19:4647–59.
32. Addison CL, Daniel TO, Burdick MD, et al. The CXC chemokine receptor 2, CXCR2, is the putative receptor for ELR$^+$ CXC chemokine-induced angiogenic activity. J Immunol 2000;165:5269–77.
33. Clark-Lewis I, Dewald B, Geiser T, Moser B, Baggiolini M. Platelet factor 4 binds to interleukin 8 receptors and activates neutrophils when its N terminus is modified with Glu-Leu-Arg. Proc Natl Acad Sci U S A 1993;90:3574–7.
34. Hebert CA, Vitangcol RV, Baker JB. Scanning mutagenesis of interleukin-8 identifies a cluster of residues required for receptor binding. J Biol Chem 1991;266:18989–94.
35. Strieter RM, Polverini PJ, Kunkel SL, et al. The functional role of the ELR motif in CXC chemokine-mediated angiogenesis. J Biol Chem 1995;270:27348–57.
36. Luster AD, Greenberg SM, Leder P. The IP-10 chemokine binds to a specific cell surface heparan sulfate site shared with platelet factor 4 and inhibits endothelial cell proliferation. J Exp Med 1995;182:219–31.
37. Wang B, Hendricks DT, Wamunyokoli F, Parker MI. A growth-related oncogene/CXC chemokine receptor 2 autocrine loop contributes to cellular proliferation in esophageal cancer. Cancer Res 2006;66:3071–7.
38. Richmond A, Lawson DH, Nixon DW, Chawla RK. Characterization of autostimulatory and transforming growth factors from human melanoma cells. Cancer Res 1985;45:6390–4.
39. Richmond A, Thomas HG. Purification of melanoma growth stimulatory activity. J Cell Physiol 1986;129:375–84.
40. Luan J, Shattuck-Brandt R, Haghnegahdar H, et al. Mechanism and biological significance of constitutive expression of MGSA/GRO chemokines in malignant melanoma tumor progression. J Leukoc Biol 1997;62:588–97.
41. Moore BB, Arenberg DA, Stoy K, et al. Distinct CXC chemokines mediate tumorigenicity of prostate cancer cells. Am J Pathol 1999;154:1503–12.
42. Zhou Y, Zhang J, Liu Q, et al. The chemokine GRO-α (CXCL1) confers increased tumorigenicity to glioma cells. Carcinogenesis 2005;26:2058–68.
43. Caunt M, Hu L, Tang T, Brooks PC, Ibrahim S, Karpatkin S. Growth-regulated oncogene is pivotal in thrombin-induced angiogenesis. Cancer Res 2006;66:4125–32.
44. Glas AS, Roos D, Deutekom M, Zwinderman AH, Bossuyt PM, Kurth KH. Tumor markers in the diagnosis of primary bladder cancer. A systematic review. J Urol 2003;169:1975–82.
45. Konety BR, Nguyen TS, Brenes G, et al. Clinical usefulness of the novel marker BLCA-4 for the detection of bladder cancer. J Urol 2000;164:634–9.
46. Lokeshwar VB, Obek C, Pham HT, et al. Urinary hyaluronic acid and hyaluronidase: markers for bladder cancer detection and evaluation of grade. J Urol 2000;163:348–56.
47. Kageyama S, Isono T, Iwaki H, et al. Identification by proteomic analysis of calreticulin as a marker for bladder cancer and evaluation of the diagnostic accuracy of its detection in urine. Clin Chem 2004;50:857–66.
48. Sheryka E, Wheeler MA, Hausladen DA, Weiss RM. Urinary interleukin-8 levels are elevated in subjects with transitional cell carcinoma. Urology 2003;62:162–6.
49. Schottenfeld D, Beebe-Dimmer J. Chronic inflammation: a common and important factor in the pathogenesis of neoplasia. CA Cancer J Clin 2006;56:69–83.
50. Michaud DS. Chronic inflammation and bladder cancer. Urol Oncol 2007;25:260–8.

FEBS Letters 582 (2008) 1444–1450

Establishment of the culture model system that reflects the process of terminal differentiation of connective tissue-type mast cells

Hirotsugu Takano[a], Shunsuke Nakazawa[a], Yasushi Okuno[b], Naritoshi Shirata[a], Sohken Tsuchiya[b], Takayuki Kainoh[a], Seigoh Takamatsu[a], Kazuyuki Furuta[a], Yoshitaka Taketomi[c], Yuko Naito[d], Hiromu Takematsu[d], Yasunori Kozutsumi[d], Gozoh Tsujimoto[b], Makoto Murakami[c,e], Ichiro Kudo[c], Atsushi Ichikawa[f], Kazuhisa Nakayama[a], Yukihiko Sugimoto[a], Satoshi Tanaka[f,g,*]

[a] *Department of Physiological Chemistry, Graduate School of Pharmaceutical Sciences, Kyoto University, Sakyo-ku, Kyoto 606-8501, Japan*
[b] *Department of Genomic Drug Discovery Science, Graduate School of Pharmaceutical Sciences, Kyoto University, Sakyo-ku, Kyoto 606-8501, Japan*
[c] *Department of Health Chemistry, School of Pharmaceutical Sciences, Showa University, 1-5-8 Hatanodai, Shinagawa-ku, Tokyo 142-8555, Japan*
[d] *Laboratory of Membrane Biochemistry and Biophysics, Graduate School of Biostudies, Kyoto University, Sakyo-ku, Kyoto 606-8501, Japan*
[e] *Tokyo Metropolitan Institute of Medical Science, 3-18-22 Honkomagome, Bunkyo-ku, Tokyo 113-8613, Japan*
[f] *Institute for Biosciences, Mukogawa Women's University, Koshien, Nishinomiya, Hyogo 663-8179, Japan*
[g] *Department of Immunobiology, School of Pharmacy and Pharmaceutical Sciences, Mukogawa Women's University, 11-68 Kyuban-cho, Koshien, Nishinomiya, Hyogo 663-8179, Japan*

Received 16 January 2008; revised 11 March 2008; accepted 20 March 2008

Available online 31 March 2008

Edited by Beat Imhof

Abstract To understand physiological roles of tissue mast cells, we established a culture system where bone marrow-derived immature mast cells differentiate into the connective tissue-type mast cell (CTMC)-like cells through modifying the previous co-culture system with Swiss 3T3 fibroblasts. Our system was found to reproducibly mimic the differentiation of CTMCs on the basis of several criteria, such as granule maturation and sensitivity to cationic secretagogues. The gene expression profile obtained by the microarray analyses was found to reflect many aspects of the differentiation. Our system is thus helpful to gain deeper insights into terminal differentiation of CTMCs.

Keywords: Mast cell; Gene expression; Differentiation; G_i

1. Introduction

Mast cells play critical roles not only in anaphylactic responses but also in modulation of diverse innate and acquired immune responses [1,2]. Mast cells originate from hematopoietic progenitor cells and undergo terminal differentiation in tissues where they are resident [3]. It is of great interest to investigate the terminal differentiation process of mast cells in each tissue, since modulation of local immune responses by mast cells should be influenced by their heterogeneity. However, little information is currently available about the heterogeneity and local maturation of tissue mast cells.

Rodent mast cells are generally classified into two populations: connective tissue mast cells (CTMCs) and mucosal mast cells (MMCs) [3,4]. CTMCs are represented by cutaneous and peritoneal mast cells and are characterized by abundant cellular histamine and heparin contents and degranulation in response to cationic secretagogues. Since recent studies demonstrated that CTMCs are involved in a wide variety of immune responses, such as autoimmunity [5], contact hypersensitivity [6], and immune tolerance [7], in addition to anaphylactic responses, detailed analysis and characterization of CTMCs are required. To establish experimental models for CTMCs, an array of attempts has been made using various sources, such as IL-3-dependent bone marrow-derived mast cells (BMMCs) [8,9] and fetal skin cells [10]. However, it remains to be clarified how immature mast cell precursors are differentiated into CTMCs and what kinds of genes regulate this process. To address these questions, we established suitable culture system to develop CTMC-like mast cells by modifying the previous methods, and thereby performed microarray analysis of the gene expression profile during the in vitro terminal differentiation of mast cells.

2. Materials and methods

2.1. Preparation of BMMCs

Specific-pathogen-free, 8–12 week-old female Balb/c mice were obtained from Japan SLC (Hamamatsu, Japan). All animal experiments were performed according to the Guidelines for Animal Experiments of Kyoto University and Mukogawa Women's University. BMMCs were prepared as described previously [11], using 10 ng/ml IL-3 (R&D Systems, Minneapolis, MN) in place of WEHI-3 conditioned medium.

2.2. Co-culture of BMMCs with fibroblasts

The co-culture system was established by modifying the previous method [12]. Swiss 3T3 fibroblasts were seeded with 50% confluency in the same RPMI-1640 medium as BMMCs, treated with 3 μg/ml mitomycin C (Sigma, St. Louis, MO) for 3 h, and further incubated for 3 h in the fresh medium without mitomycin C. BMMCs

*Corresponding author. Address: Department of Immunobiology, School of Pharmacy and Pharmaceutical Sciences, Mukogawa Women's University, 11-68 Kyuban-cho, Koshien, Nishinomiya, Hyogo 663-8179, Japan. Fax: +81 798 41 2792.
E-mail address: s_tanaka@mukogawa-u.ac.jp (S. Tanaka).

Abbreviations: BMMC; bone marrow-derived mast cell; CTMC; connective tissue mast cell; MMC; mucosal mast cell

0014-5793/$34.00 © 2008 Published by Elsevier B.V. on behalf of the Federation of European Biochemical Societies.
doi:10.1016/j.febslet.2008.03.033

(5×10^5 cells/ml) were seeded onto this Swiss 3T3 feeder cells and culture for 4 days in the presence of 100 ng/ml stem cell factor (SCF), which was supplied as the conditioned medium of Sf9 cells infected with the recombinant baculovirus encoding murine SCF [12]. An equal volume of the fresh medium containing 100 ng/ml SCF was added at Day-2. When the feeder cells were replaced at Day-4, whole culture was trypsinized and the contaminating fibroblasts were removed as the adhered cells through repeated plating.

2.3. Protease assay

Mast cells were washed with PBS, lysed in PBS containing 2 M NaCl and 0.5% Triton X-100, and incubated for 30 min on ice. The lysate was centrifuged at $10000 \times g$ for 30 min at 4 °C. Activities of three different types of granule proteases in the resultant supernatants were measured using their specific chromogenic peptide substrates, such as S-2586 (tryptic), S-2288 (chymotryptic), and M-2245 (carboxypeptidase A) [13].

2.4. Degranulation

Mast cells were washed with PIPES buffer (25 mM PIPES–NaOH, pH 7.4, containing 125 mM NaCl, 2.7 mM KCl, 5.6 mM glucose, 1 mM $CaCl_2$, and 0.1% bovine serum albumin) and incubated with the buffer containing compound 48/80 (10 μg/ml, Sigma), substance P (100 μM, Sigma), or A23187 (1 μM, Calbiochem, Darmstadt, Germany) for 30 min. In case of antigen stimulation, mast cells sensitized with 1 μg/ml an anti-DNP IgE (SPE-7, Sigma) for 6 h were stimulated with 30 ng/ml DNP-human serum albumin (Sigma). Degranulation was evaluated by measuring β-hexosaminidase activity.

2.5. Oligonucleotide microarray

Total cellular RNAs were isolated from mast cells using an RNeasy mini kit (QIAGEN, Valencia, CA) according to the manufacturer's instructions. Target RNAs were prepared following technical recommendations found in the Affymetrix Gene Chip Expression Analysis Technical Manual (Affymetrix, Santa Clara, CA). The obtained RNAs were labeled and hybridized to the 430A murine GeneChip (Affymetrix), which contains the oligonucleotide probe set for approximately 22000 genes. We used the RMA (robust multi-array analysis) [14] expression measure that represents the log transform of (background corrected and normalized) intensities of the GeneChips. The RMA measures were computed using the R package program, which is freely available on the web site (http://www.bioconductor.org). We then removed all genes whose maximum minus minimum values were less than 2 (2-fold change), and selected 1315 genes, which were differentially expressed between the cells during co-culture. Using the *k*-means clustering algorithm, these genes were classified into 10 clusters on the basis of similarity of their expression profiles.

2.6. Flow cytometry

The surface expression levels of FcεRI were determined as described previously [15]. For measuring the surface expression of IL-17Rs, mast cells were pretreated with 2.4G2 (BD Biosciences, San Diego, CA) were then treated with 20 μg/ml IL-17 (R&D Systems) at 4 °C for 60 min. Labeling of the cells was performed by incubation with a phycoerythrin (PE)-conjugated anti-mouse IL-17 antibody (BD Biosciences) at 4 °C for 10 min. For measuring the expression of ICAM-1, c-kit, or CD81, FITC-conjugated anti-ICAM-1, PE-conjugated anti-c-kit, or anti-CD81 antibody (BD Biosciences) was used, respectively.

2.7. Immunoblot analyses

Immunoblot analysis was performed as described previously [11] using antibodies raised against actin, $G\alpha_{i3}$ (Chemicon, Temecula, CA), $G\alpha_{i1}$, Itk (Upstate Biotechnology, Charlottesville, VA), $G\alpha_{i2}$, COX-2, GATA-1, c-Myb, Tiam1, Lyn (Santa Cruz, CA), and COX-1 (Cayman Chemicals, Ann arbor, MI).

2.8. Measurement of cytosolic Ca^{2+} concentrations

Cytosolic Ca^{2+} concentrations were measured using Fura-2/AM as described previously [11].

2.9. Purification of peritoneal mast cells

Peritoneal mast cells were purified by means of MACS system in accordance with the manufacturer's instruction (Miltenyi Biotech, Bergisch Gladbach, Germany). Briefly, mast cells were enriched using the magnet-conjugated anti-c-kit antibody after depletion of the other cell lineages using the antibodies against CD11b, CD45R, CD90, and Ter119. The purity of mast cells was greater than 98% based on the Safranin staining.

3. Results and discussion

3.1. Changes in granule staining properties, protease activities, and histamine content of cultured mast cells

We found in the preliminary experiments that the previously reported co-culture methods to develop CTMC-like cells have room for improvement in reproducibility. Since mast cells can affect growth of the feeder fibroblasts and vice versa [16], a slight change of the culture condition can lead to imbalance of the number of mast cells and fibroblasts, which often affects the process of maturation. We employed the mitomycin C treatment to exclude such instability in the co-culture system. Our method exhibited several advantages over the reported methods using 3T3 fibroblasts, in particular in terms of high reproducibility and expandability, which allowed us to investigate the changes over time. Although at Day-0, the majority of cells (>90%) were stained with Alcian blue but not with Safranin, the population of Safranin-positive mast cells was gradually increased up to ~80% at Day-16 of the co-culture (Fig. 1A). It is generally accepted that an increase in histamine content and granule protease expression reflects maturation of mast cells [17]. All the three kinds of granule protease activities and the cellular histamine content were found to be gradually increased (Fig. 1B–E). High levels of FcεRI and c-kit were detected on the surface of more than 95% of the cultured mast cells throughout the co-culture period (Fig. 1F, and data not shown).

A recent study described the generation of a large number of high-purity CTMC-like mast cells from mouse fetal skin cells [10]. Embryonic stem cell–derived mast cells have also been found to be a good model for CTMCs [18]. However, it was difficult to investigate the changes during mast cell maturation using these culture methods, since differentiation and maturation of mast cells from progenitors occurs concurrently with elimination of the other cell lineages. In contrast, we used BMMCs, the vast majority of which expresses both c-kit and FcεRI, as the initial population to develop mature mast cells. The changes observed in our system are therefore attributed solely to those in the mast cell lineage.

3.2. Gene expression profile during maturation of cultured mast cells

The characterization of the co-cultured mast cells suggested that our system reflected the process of terminal differentiation of CTMCs. We therefore performed the microarray analysis of gene expression in the cultured mast cells to gain a deeper appreciation on this process at the molecular levels. The number of genes, of which expression levels represent greater than 2-fold change, was 1315. These genes were classified into 10 groups by the clustering analysis (Fig. 2 and Supplementary data).

Expression profiles of several genes appeared to correlate well with characteristic changes concomitant with mast cell maturation. (i) The drastic induction of mast cell protease genes (*Mcpt*) is consistent with the increase in tryptic and chymotryptic activ-

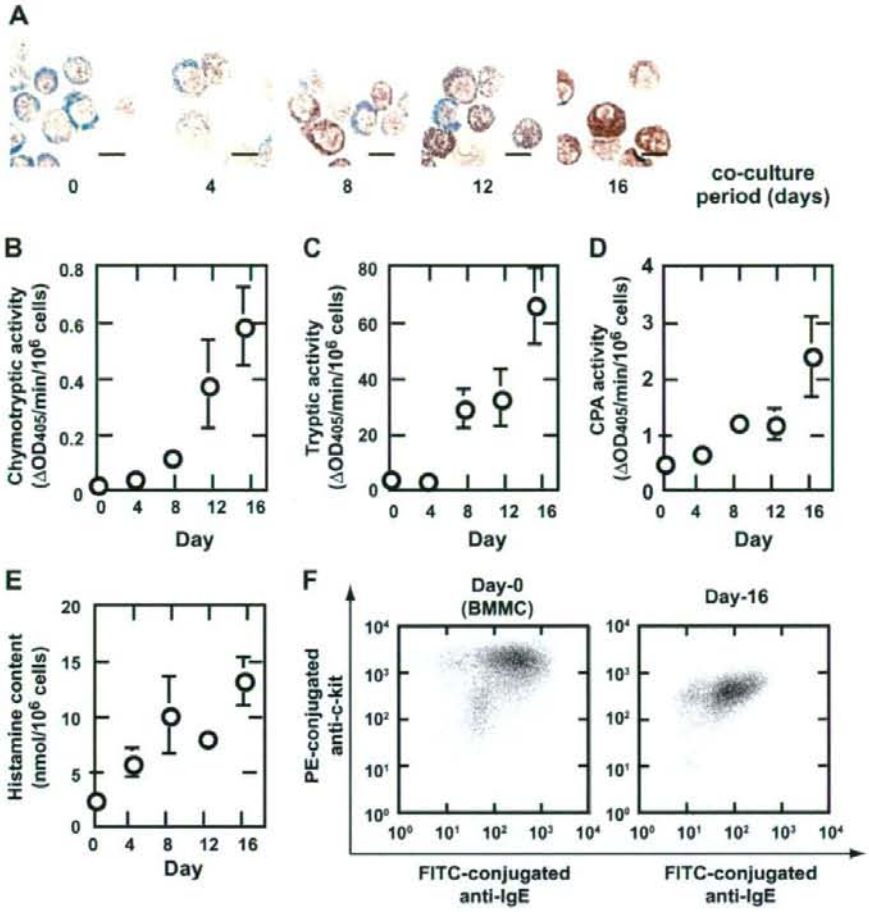

Fig. 1. Maturation of BMMCs co-cultured with fibroblasts in the presence of SCF. (A) BMMCs co-cultured for 16 days were collected (Day-0, -4, -8, -12, and -16) and stained with Alcian blue and Safranin-O. Bars = 10 μm. (B–E) Granule protease activities of the cells were measured (B: chymotryptic activity, C: tryptic activity, D: carboxypeptidase A activity). Histamine content was also measured (E). Values are presented by the means ± S.E.M. (n = 5). (F) Surface expression of FcεRI and c-kit was determined by flow cytometry.

ities (Fig. 1B and C). In addition, induction of other protease genes, such as cathepsin B (*Ctsb*) and transmembrane tryptase (*Tpsg1*), was also observed. (ii) Induction of histidine decarboxylase (*Hdc*), which catalyzes histamine synthesis, is also consistent with the increase in cellular histamine content (Fig. 1E). (iii) Heparan sulfate biosynthesis is mediated by an array of enzymes [19]. We found the increased gene expression of these enzymes, including exostoses 1 (*Ext1*), and heparan sulfate 6-*O*-sulfotransferase 2 (*Hs6st2*), which mediates synthesis of polysaccharide backbone and 6-*O*-sulfation after *N*-deacetylation and *N*-sulfation of *N*-acetyl glucosamine, respectively. Glucosaminyl *N*-deacetylase/*N*-sulfotransferase-2 (*Ndst2*) is known to be essential for heparin biosynthesis in mast cells, and peritoneal mast cells in the NDST-2-deficient mice exhibit aberrant granule morphology and decreased granule proteases [13,20]. However, we unexpectedly found a decrease in the *NDST-2* gene expression during maturation. Analysis of these enzymes at the protein level is surely required to address this inconsistency. (iv) As for arachidonic acid metabolism, up-regulation of hematopoietic prostaglandin (PG) D synthase (*Ptgds2*) and down-regulation of leukotriene (LT) C_4 synthase (*Ltc4s*) are consistent with the previous report indicating the production of PGD_2 in preference to LTC_4 in CTMCs [17]. Given that CTMCs adhere to the extracellular matrix in the tissues, it is interesting that up-regulation of the genes related to adhesion, such as integrins (*Itga5*, *Itga9*, and *Itgb1*), CD44 (*Cd44*), and ICAM-1 (*Icam1*), was detected during the co-culture period. Altogether, these changes in the gene expression are in good accordance with phenotypic changes observed during mast cell maturation, indicating that our culture system successfully mimics the maturation process.

Immunoblot analyses confirmed that the changes in the expression of various proteins paralleled those of the corresponding gene expression in the microarray analyses (Fig. 2A and B). GATA-1 and GATA-2 were reported to be required for mast cell differentiation [21,22]. Recently, Masuda et al. demonstrated that these transcription factors are required for maintaining mast cell-specific gene expression and are required

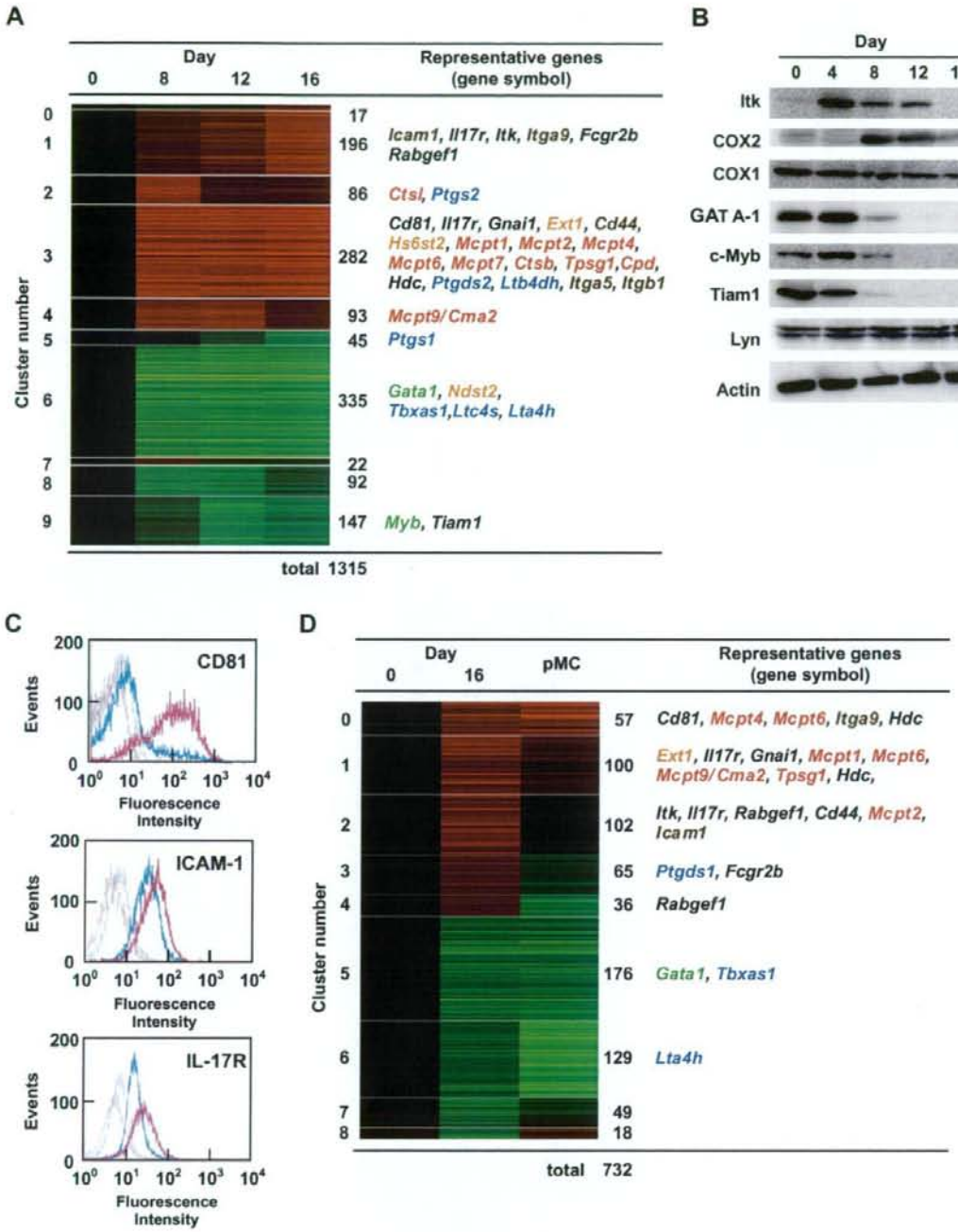

Fig. 2. Clustering analysis of the gene expression profile during maturation of cultured mast cells. (A) Co-cultured mast cells were subjected to analysis of the gene expression profiles using microarray (Affymetrix, 430A murine GeneChip, ~22000 genes). Selected 1315 genes, of which maximum minus minimum expression values were greater than 2 (2-fold change), were classified into 10 clusters on the basis of similarity in the expression profiles and presented by the columns (red: increased, green: decreased). The number of genes and the representative genes (proteases; red, enzymes related to arachidonate metabolism; blue, adhesion molecules; brown, enzymes related to heparin synthesis; orange, and transcription factors; green) in each cluster are indicated on the right. (B) The results of immunoblot analyses of the selected proteins are presented. Immunoblot analyses for Lyn and actin were performed as the loading control. (C) Surface expression of CD81, ICAM-1, and IL-17Rs was investigated by flow cytometry in BMMCs (blue lines) and co-cultured mast cells (Day-16, red lines). The isotype controls were shown by the dotted lines. (D) BMMCs (Day-0), Day-16 co-cultured mast cells (Day-16), and peritoneal c-kit$^+$ cells (pMC) were subjected to analysis of the gene expression profiles using microarray (430A murine GeneChip). Selected 732 genes, of which differences in expression values were greater than 2 between Day-0 and Day-16 co-cultured mast cells, were classified into 9 clusters on the basis of similarity in the expression profiles. The number of genes and the representative genes in each cluster are indicated.

for activation upon IgE-mediated antigen stimulation [23]. We observed, however, a drastic GATA-1 down-regulation during the later stage of co-culture period (Fig. 2B), indicating that GATA-1 may be dispensable for the final step of mast cell maturation.

We then analyzed expression of several membrane proteins, including CD81, ICAM-1, and the IL-17 receptor (IL-17R), by flow cytometry (Fig. 2C). *CD81* was one of the strikingly up-regulated genes during the co-culture period (supplemental data). Since Yamada et al. demonstrated that the higher surface expression of CD81 is one of the signatures of cutaneous mast cells [10], it is likely that the drastic up-regulation at Day-16 reflects the differentiation towards CTMC-like cells. The surface expression of ICAM-1 was also confirmed to be up-regulated in the Day-16 cultured mast cells. Consistent with induction of the IL-17R gene on the microarray analysis (Fig. 2A, clusters #1 and #3, *Il17r*), the surface expression of IL-17R, which was detectable on BMMCs, was significantly up-regulated in the Day-16 cultured mast cells. Nakae et al. demonstrated that IL-17 enhanced ionomycin-induced TNF-α production in BMMCs, although IL-17 alone failed to induce TNF-α [24]. IL-17R may determine the sensitivity to IL-17 in mature tissue mast cells. Our results indicate that these membrane proteins are good candidates for the surface marker of CTMCs.

3.3. Comparison of gene expression profiles between cultured mast cells and peritoneal mast cells

We compared the gene expression profile of the Day-16 co-cultured mast cells with that of peritoneal mast cells, which are regarded as typical CTMCs. The characteristic changes in gene expression profile between the Day-0 and Day-16 co-cultured mast cells were also confirmed in the case of the comparison between BMMCs (Day-0) and peritoneal mast cells; approximately 70% of the extracted genes (511 genes in 732 genes; parallel increase in clusters 0 and 1, parallel decrease in clusters 5, 6, and 7), of which differences in expression values were greater than 2-fold between Day-0 and Day-16 co-cultured mast cells, exhibited similar trends in the peritoneal mast cells (Fig. 2D). This result suggests that the approach with the co-culture system can efficiently select the genes, of which expression is characteristic of CTMCs.

3.4. Degranulation of cultured mast cells in response to cationic secretagogues

BMMCs and the co-cultured mast cells responded to IgE-mediated antigen stimulation in a similar fashion up to Day-12 (Fig. 3A). A significant decrease in degranulation was found at Day-16, which may be attributed to up-regulation of the molecules that can suppress activation of mast cells upon IgE-mediated antigen stimulation, such as FcγRIIB, Rab-GEF1, and CD81 (Fig. 2A, clusters #1 and #3) [25–27]. The constant levels of degranulation in response to a Ca^{2+} ionophore, A23187, were observed, indicating that the process of Ca^{2+} influx-mediated degranulation was not affected during the co-culture period (Fig. 3B).

CTMCs can be distinguished from MMCs or BMMCs in their sensitivity to cationic secretagogues, such as compound 48/80. At Day-16, the cultured mast cells released 60% and 40% of β-hexosaminidase activity in response to compound 48/80 and substance P, respectively, whereas no or little release

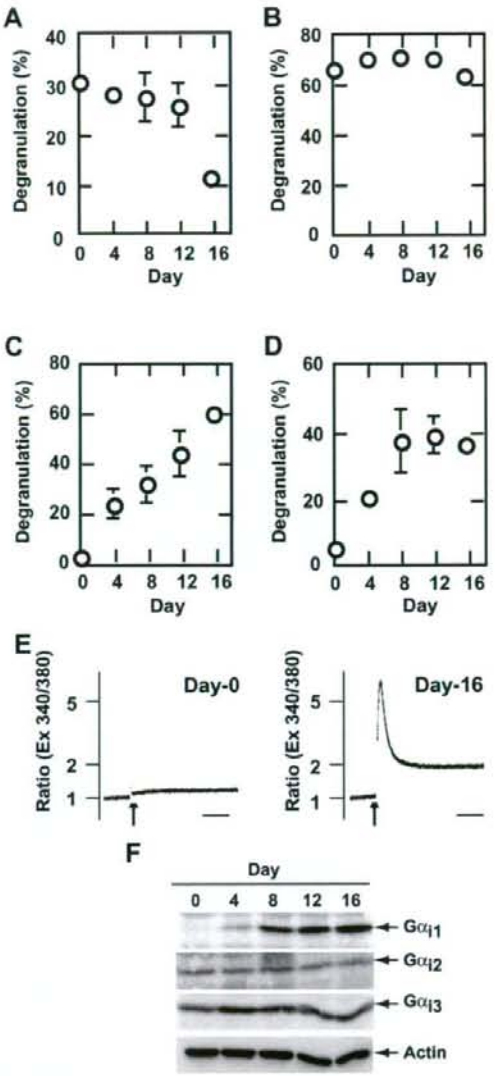

Fig. 3. Cationic secretagogue-induced degranulation and $G_{\alpha i}$ expression. (A–D) Co-cultured mast cells were separated and stimulated with 1 μM A23187 (B), 10 μg/ml compound 48/80 (C), or 100 μM substance P (D). In case of IgE-mediated antigen stimulation, the sensitized mast cells were stimulated with the antigen as described in Section 2 (A). Values are presented by the means ± S.E.M. ($n = 5$). (E) Intracellular Ca^{2+} mobilization was monitored using Fura-2/AM. BMMCs (Day-0) and co-cultured mast cells (Day-16) were stimulated with 10 μg/ml compound 48/80 (indicated by the arrows). These are the representatives of three similar independent experiments. Bars = 1 min. (F) Expression of three $G_{\alpha i}$ subtypes in the co-cultured mast cells at each time point was examined by immunoblot analyses. An anti-actin antibody was used as a loading control.

from BMMCs (Day-0) was detected (Fig. 3C and D). Since a previous study demonstrated that compound 48/80 causes intracellular Ca^{2+} mobilization in mast cells [28], we then examined cytosolic Ca^{2+} response to the secretagogue. As expected, compound 48/80 increased the cytosolic Ca^{2+} concentrations in

the Day-16 cultured mast cells, but not in BMMCs (Day-0) (Fig. 3E).

Degranulation induced by basic secretagogues was reported to be mediated by the heterotrimeric G protein, G_i, especially by G_{i3}, in rat peritoneal mast cells [29]. Ferry et al. suggested that the $\beta\gamma$ subunits of G_{i2} and G_{i3} induced degranulation through activating phospholipase Cβ [30]. Furthermore, a recent study using cultured human mast cells revealed that the $G\alpha_{i3}$ protein was induced upon co-culture with 3T3 fibroblasts and suggested an involvement of G_{i3} in eosinophil major basic protein-induced degranulation [31]. We then examined the levels of three $G_{\alpha i}$ subtypes (Fig. 3F). In good agreement with the microarray results (Fig. 2A, cluster #3, *Gnai1*), the level of the $G_{\alpha i1}$ protein was drastically increased during the co-culture period, whereas the level of $G_{\alpha i2}$ or $G_{\alpha i3}$ was not significantly changed. Furthermore, the $G\alpha_{i1}$ induction is well correlated with the elevated degranulation in response to compound 48/80 (Fig. 3C). Previous studies using basic secretagogues have paid little attention to the $G\alpha_{i1}$ protein, since they mostly used rat peritoneal mast cells, which lack the expression of $G\alpha_{i1}$. Our results suggest that $G\alpha_{i1}$ is a potent candidate for the regulator of basic secretagogue-induced degranulation in mouse mast cells.

3.5. Conclusion

In summary, we succeeded in improving the culture system to develop the CTMC-like mast cells. This system allows us to investigate the gene expression profiles during maturation of mast cells, which should contribute to understanding the mechanism underlying mast cell terminal differentiation.

Acknowledgements: This study was supported in part by 21st Century COE Program "Knowledge Information Infrastructure for Genome Science", a grant from Uehara Memorial Foundation, Naito Foundation, Kao Foundation for Arts and Sciences, Sankyo Foundation of Life Science, and by Grants-in-Aid for Scientific Research from the Ministry of Education, Culture, Science, Sports and Technology of Japan and from the Ministry of Health and Labor of Japan.

Appendix A. Supplementary data

Supplementary data associated with this article can be found, in the online version, at doi:10.1016/j.febslet.2008.03.033.

References

[1] Metz, M., Grimbaldeston, M.A., Nakae, S., Piliponsky, A.M., Tsai, M. and Galli, S.J. (2007) Mast cells in the promotion and limitation of chronic inflammation. Immunol. Rev. 217, 304–328.
[2] Metz, M. and Maurer, M. (2007) Mast cells-key effector cells in immune responses. Trends Immunol. 28, 234–241.
[3] Kitamura, Y. (1989) Heterogeneity of mast cells and phenotypic change between subpopulations. Annu. Rev. Immunol. 7, 59–76.
[4] Stevens, R.L. and Austen, K.F. (1989) Recent advances in the cellular and molecular biology of mast cells. Immunol. Today 10, 381–386.
[5] Benoist, C. and Mathis, D. (2002) Mast cells in autoimmune disease. Nature 420, 875–878.
[6] Bryce, P.J., Miller, M.L., Miyajima, I., Tsai, M., Galli, S.J. and Oettgen, H.C. (2004) Immune sensitization in the skin is enhanced by antigen-independent effects of IgE. Immunity 20, 381–392.
[7] Lu, L.F., Lind, E.F., Gondek, D.C., Bennett, K.A., Gleeson, M.W., Pino-Lagos, K., Scott, Z.A., Coyle, A.J., Reed, J.L., Van Snick, R.J., Strom, T.B., Zheng, X.X. and Noelle, R.J. (2006) Mast cells are essential intermediaries in regulatory T-cell tolerance. Nature 442, 997–1002.
[8] Levi-Schaffer, F., Austen, K.F., Gravallese, P.M. and Stevens, R.L. (1986) Coculture of interleukin 3-dependent mouse mast cells with fibroblasts results in a phenotypic change of the mast cells. Proc. Natl. Acad. Sci. USA 83, 6485–6488.
[9] Dayton, E.T., Pharr, P., Ogawa, M., Serafin, W.E., Austen, K.F., Levi-Schaffer, F. and Stevens, R.L. (1988) 3T3 fibroblasts induce cloned interleukin 3-dependent mouse mast cells to resemble connective tissue mast cells in granular constituency. Proc. Natl. Acad. Sci. USA 85, 569–572.
[10] Yamada, N., Matsushima, H., Tagaya, Y., Shimada, S. and Katz, S.I. (2003) Generation of a large number of connective tissue type mast cells by culture of murine fetal skin cells. J. Invest. Dermatol. 121, 1425–1432.
[11] Tanaka, S., Takasu, Y., Mikura, S., Satoh, N. and Ichikawa, A. (2002) Antigen-independent induction of histamine synthesis by immunoglobulin E in mouse bone marrow-derived mast cells. J. Exp. Med. 196, 229–235.
[12] Ogasawara, T., Murakami, M., Suzuki-Nishimura, T., Uchida, M.K. and Kudo, I. (1997) Mouse bone marrow-derived mast cells undergo exocytosis, prostanoid generation, and cytokine expression in response to G protein-activating polybasic compounds after coculture with fibroblasts in the presence of c-kit ligand. J. Immunol. 158, 393–404.
[13] Forsberg, E., Pejler, G., Ringvall, M., Lunderius, C., Tomasini-Johansson, B., Kusche-Gullberg, M., Eriksson, I., Ledin, J., Hellman, L. and Kjellén, L. (1999) Abnormal mast cells in mice deficient in a heparin-synthesizing enzyme. Nature 400, 773–776.
[14] Irizarry, R.A., Bolstad, B.M., Collin, F., Cope, L.M., Hobbs, B. and Speed, T.P. (2003) Summaries of Affymetrix GeneChip probe level data. Nucleic Acids Res. 31, e15.
[15] Tanaka, S., Mikura, S., Hashimoto, E., Sugimoto, Y. and Ichikawa, A. (2005) Ca^{2+} influx-mediated histamine synthesis and IL-6 release in mast cells activated by monomeric IgE. Eur. J. Immunol. 35, 460–468.
[16] Dayton, E.T., Caulfield, J.P., Hein, A., Austen, K.F. and Stevens, R.L. (1989) Regulation of the growth rate of mouse fibroblasts by IL-3-activated mouse bone marrow-derived mast cells. J. Immunol. 42, 4307–4313.
[17] Metcalfe, D.D., Baram, D. and Mekori, Y. (1997) Mast cells. Physiol. Rev. 77, 1033–1079.
[18] Tsai, M., Wedemeyer, J., Ganiatsas, S., Tam, S.Y., Zon, L.I. and Galli, S.J. (2000) In vivo immunological function of mast cells derived from embryonic stem cells: an approach for the rapid analysis of even embryonic lethal mutations in adult mice in vivo. Proc. Natl. Acad. Sci. USA 97, 9186–9190.
[19] Kusche-Gullberg, M. and Kjellén, L. (2003) Sulfotransferase in glycosaminoglycan biosynthesis. Curr. Opin. Struct. Biol. 13, 605–611.
[20] Humphries, D.E., Wong, G.W., Friend, D.S., Gurish, M.F., Qiu, W.-T., Huang, C., Sharpe, A.H. and Stevens, R.L. (1999) Heparin is essential for the storage of specific granule proteases in mast cells. Nature 400, 769–772.
[21] Walsh, J.C., DeKoter, R.P., Lee, H.J., Smith, E.D., Lancki, D.W., Gurish, M.F., Friend, D.S., Stevens, R.L., Anastasi, J. and Singh, H. (2002) Cooperative and antagonistic interplay between PU.1 and GATA-2 in the specification of myeloid cell fates. Immunity 17, 665–676.
[22] Migliaccio, A.R., Rana, R.A., Sanchez, M., Lorenzini, R., Centurione, L., Bianchi, L., Vannucchi, A.M., Migliaccio, G. and Orkin, S.H. (2003) GATA-1 as a regulator of mast cell differentiation revealed by the phenotype of the GATA-1^{low} mouse mutant. J. Exp. Med. 197, 281–296.
[23] Masuda, A., Hashimoto, K., Yokoi, T., Doi, T., Kodama, T., Kume, H., Ohno, K. and Matsuguchi, T. (2007) Essential role of GATA transcription factors in the activation of mast cells. J. Immunol. 178, 360–368.
[24] Nakae, S., Suto, H., Berry, G.J. and Galli, S.J. (2007) Mast cell-derived TNF can promote Th17 cell-dependent neutrophil recruitment in ovalbumin-challenged OTII mice. Blood 109, 3640–3648.
[25] Malbec, O. and Daeron, M. (2007) The mast cell IgG receptors and their roles in tissue inflammation. Immunol. Rev. 217, 206–221.

[26] Fleming, T.J., Donnadieu, E., Song, C.H., Laethem, F.V., Galli, S.J. and Kinet, J.P. (1997) Negative regulation of FceRI-mediated degranulation by CD81. J. Exp. Med. 186, 1307–1314.

[27] Tam, S.Y., Tsai, M., Snouwaert, J.N., Kalesnikoff, J., Scherrer, D., Nakae, S., Chatterjea, D., Bouley, D.M. and Galli, S.J. (2004) RabGEF1 is a negative regulator of mast cell activation and skin inflammation. Nat. Immunol. 5, 844–852.

[28] Senyshyn, J., Baumgartner, R.A. and Beaven, M.A. (1998) Quercetin sensitizes RBL-2H3 cells to polybasic mast cell secretagogues through increased expression of G_i GTP-binding proteins linked to a phospholipase C signaling pathway. J. Immunol. 160, 5136–5144.

[29] Aridor, M., Rajmilevich, G., Beaven, M.A. and Sagi-Eisenberg, R. (1993) Activation of exocytosis by the heterotrimeric G protein G_{i3}. Science 262, 1569–1572.

[30] Ferry, X., Eichwald, V., Daeffler, L. and Landry, Y. (2001) Activation of $\beta\gamma$ subunits of G_{i2} and G_{i3} proteins by basic secretagogues induces exocytosis through phospholipase Cβ and arachidonate release through phospholipase Cγ in mast cells. J. Immunol. 167, 4805–4813.

[31] Piliponsky, A.M., Gleich, G.J., Nagler, A., Bar, I. and Levi-Schaffer, F. (2003) Non-IgE-dependent activation of human lung- and cord blood-derived mast cells is induced by eosinophil major basic protein and modulated by the membrane form of stem cell factor. Blood 101, 1898–1904.

—Reviews—

バイオインフォマティクスとケモインフォマティクスの融合によるインシリコ創薬研究

奥野恭史

In silico Drug Discovery Based on the Integration of Bioinformatics and Chemoinformatics

Yasushi OKUNO

Department of PharmacoInformatics, Centre for Integrative Education of Pharmacy Frontier, Graduate School of Pharmaceutical Sciences, Kyoto University, 46-29 Yoshida Shimoadachi-cho, Sakyo-ku, Kyoto 606-8501, Japan

(Received May 28, 2008)

With the near completion of the human genome sequencing, bioinformatics and chemoinformatics are expected as promising tools in genome-based drug discovery. The emerging field of chemical genomics is accumulating large-scale assay data on compound-protein interactions. We are now developing new mining methods for the chemical genomics data based on the integration of bioinformatics and chemoinformatics. Here we present a GPCR-ligand database (GLIDA) and a novel *in silico* screening method, which we have developed. GLIDA is a novel public GPCR-related chemical genomics database that is primarily focused on the correlation of information between GPCRs and their ligands. Our *in silico* screening method is based on statistical machine learning of the conserved patterns of molecular recognition extracted from comprehensive compound-protein interaction data. These are promising approaches to accelerating drug discovery processes.

Key words——chemoinformatics; bioinformatics; *in silico* screening

1. はじめに

ヒトゲノムが解読された今日，莫大なゲノム情報から創薬への手掛かりを発見すること，すなわち「ゲノム創薬」に大きな期待が寄せられている．ゲノム創薬は，ゲノム情報を出発点とし創薬の標的遺伝子探索からリード化合物探索を経て臨床段階に至る広範で高度に専門化した複合領域であり，その実践にはこれらの複合領域の橋渡しを実現する統合的なインフォマティクス基盤「創薬インフォマティクス」が必須となる．われわれは，創薬インフォマティクスという新たな研究分野の創成に向け，バイオ情報を扱うバイオインフォマティクスとケミカル情報を扱うケモインフォマティクスという独立に発展してきた2つの情報科学分野の統合を図り，バイオ情報とケミカル情報の両者を同時に統合的にマイニングする新しい情報技術の開発に着手している．なお本研究は，現在，国内外で注目されているケミカルゲノミクス・ケミカルバイオロジーのための有力な情報基盤ともなり得るものと考えられる．

京都大学大学院薬学研究科統合薬学フロンティア教育センター（〒606-8501 京都市左京区吉田下阿達町 46-29)
e-mail: okuno@pharm.kyoto-u.ac.jp

本総説は，平成20年度日本薬学会奨励賞の受賞を記念して記述したものである．

2. ケミカル空間とケミカルゲノミクス

2004年12月のNature誌において，Chemical Space特集号が発表された.[1] そこでは，化合物の種類は10^{60}個を超える天文学的なバリエーションを有しており，化合物空間を探索することは宇宙探索と同様に壮大な課題であることが提示されている．このことは医薬品の候補化合物となり得る新規な活性化合物を見つけ出すことがいかに困難でセレンディップなことであるかを示唆するものである．

これらケミカル空間の探索の基礎研究としてケミカルゲノミクス・ケミカルバイオロジー研究が近年注目されている．ケミカルゲノミクスでは，その命題として「莫大な数の化合物と生体系（タンパク質や細胞など）との相互作用を包括的に明らかにする

こと」が挙げられている．実際，米国では，ケミカルゲノミクスプロジェクトを掲げ，数百万もの膨大な化合物に関する情報を収集し，有用化合物の探索に国策として取り組んでいる．

しかしながら，広大な化合物空間から生物活性を有する化合物を探し当てる化合物探索には，天文学的な数量に対応できる新たなインフォマティクス技術とハイスループット技術の研究開発が必須である．そこで，われわれは，莫大な化合物群とタンパク質群との相互作用様式をゲノムスケールで解析することを目的とした情報学的技術，すなわちケミカルゲノミクスのためのインフォマティクス技術の研究開発を行っている．

3. ケモインフォマティクスとバイオインフォマティクス

ケミカルゲノミクス・ケミカルバイオロジーでは，化合物のケミカル情報と生体系のバイオ情報の2種の異なる情報が対象となる．したがって，ケミカルゲノミクスのための情報処理技術には，ケミカル情報を処理するケモインフォマティクスとバイオ情報を処理するバイオインフォマティクスを融合する新たなインフォマティクス技術の開発が必須となる．しかしながら，化学と生物学という異なる分野を背景に持つ2つのインフォマティクスは，独立して発展してきており現状では互いに相容れない．そこで，われわれはケモインフォマティクスとバイオインフォマティクスにおける方法論的なアナロジーに着目しその融合を図った．すなわち，ケモインフォマティクスもバイオインフォマティクスもともに，個体（化合物やタンパク質）の特徴量を数値やベクトルで表現することにより，各個体の相対的な特性の違いを探索空間上の個体間の距離として定量的に算出する方法論を基本としている．例えば，ケモインフォマティクスでは，データベースに集積された膨大な化合物エントリーは化学構造や特性を定量的に表すベクトルとして表現され，その相対的な違いを距離の尺度として持つ座標空間（探索空間）をコンピュータ内部に構築する．データベース検索はこの探索空間において距離が近接する化合物を類似化合物として選出してくることになる．また，バイオインフォマティクスでも同様の考え方であり，遺伝子・タンパク質エントリーは配列や構造として表現され，それぞれの相同性（類似度）を尺度として持つ探索空間（バイオデータの場合，探索空間は系統樹やネットワーク構造になっている場合もある）が構築され，データベース検索にはこの探索空間に基づき，類似（類縁）遺伝子・タンパク質が選出される．

一方，ケミカルゲノミクスとは，ケミカル空間の個体（化合物）とバイオ空間の個体（遺伝子・タンパク質）との相互作用関係を網羅的に明らかにする研究であり，Fig. 1の赤線に示す対応関係を付加したモデルであると考えられる．ここで，われわれは，ケミカル情報とバイオ情報を統合的に処理するために，ケミカル空間（緑色）とバイオ空間（黄色）を独立して扱うのではなく，2つの空間を融合したモデルをケミカルゲノミクスのためのインフォマティクスモデルとして考案した．

4. ケミカル空間とバイオ空間の融合モデル

情報科学的アプローチによる化合物探索は，これまで化合物のケミカル情報のみを用いたケモインフォマティクス手法が用いてきた．これに対し，われわれの手法は，このケミカル情報のみの従来手法にバイオインフォマティクス技術を融合させ，バイオ情報を考慮に入れた化合物探索を実現する新しいインフォマティクス手法と言える（Fig. 1）．

例えば，化合物について構造や特性の類似性を相対的な位置関係として表現したものをケミカル空間（赤が化合物，緑領域がケミカル空間）として定義するとともに，タンパク質についても類似関係（配列や構造の相同性）を相対的な位置関係として表現したものをバイオ空間（青がタンパク質，黄色領域がバイオ空間）として定義する．さらに個々の化合物とタンパク質の結合をリンク（黒線）することによって，これらケミカル空間とバイオ空間を融合した単純なモデルを構築できる（Fig. 2）．

ここで，標的タンパク質に作用する化合物候補を探索する *In silico* スクリーニングにこの融合モデルを適用する場合を考えると，

1） 標的タンパク質（青星）の配列構造から，そのタンパク質がバイオ空間座標にマッピングされる．

2） バイオ空間にマッピングされた標的タンパク質の近隣タンパク質からのケミカル空間へのリンク情報をたどること（青矢印）により，その標的タンパク質が関係するケミカル空間のエリア（青円内）を指定することができる．

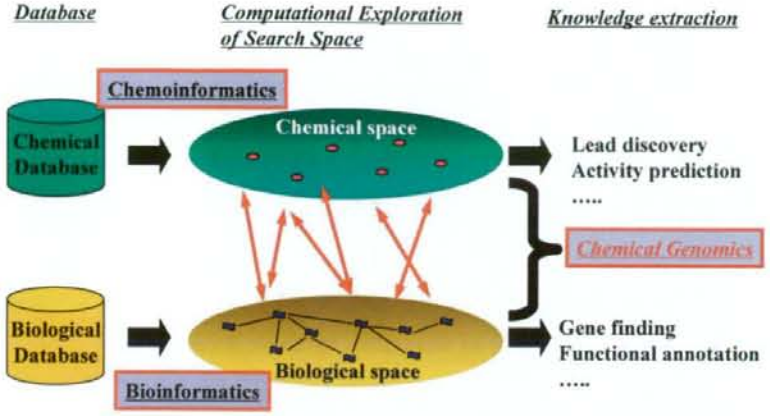

Fig. 1. Bioinformatics and Chemoinformatics

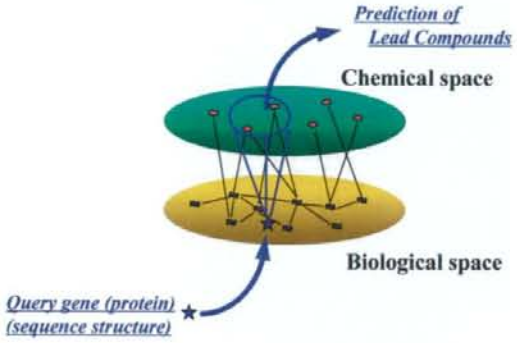

Fig. 2. *In silico* Screening for Chemical Genomics Data

3) 上記エリア内の化合物群が，標的タンパク質に相互作用する可能性のある化合物群と推定される（ここでは，類似のタンパク質は，類似の化合物を結合するという前提を基にしている）．

われわれは，このケミカル空間とバイオ空間の融合モデルを用いた探索を，GPCR ファミリーとそのリガンド化合物の探索に適用し，GLIDA データベース[2-4]として Web サービスを行っている．GLIDA は，GPCR のバイオ情報，そのリガンドのケミカル情報，及び GPCR とリガンドの相互作用情報の 3 種類の情報より構成されている．GPCR のエントリーはヒト，ラット，マウスに限定し，バイオ情報は GPCRDB から取得した．また，GPCR と結合するリガンドのエントリーとそのケミカルデータ（化学名，構造式，分子量，MDL Mol ファイルなど）は IUPHAR Receptor Database, PubMed, PubChem 及び MDL ISIS/Base 2.5 などの公共又は商用のデータベースから取得した．具体的には，2008 年 1 月現在，24077 件のリガンドエントリー，及び 39140 件のリガンド–GPCR の相互作用エントリーの登録に至っている．

各エントリーの検索は，GPCR（またはリガンド）のキーワード検索及びクラス分類テーブルから行うことが可能である．ここで，GPCR 分類は，GPCRDB に定義されている進化系統樹由来の分類に従っている．またリガンド分類は，KEGG で定義されている原子タイプの原子数／結合数に基づいた頻度プロファイルから距離行列を計算し，主成分分析（PCA）に基づいて GLIDA 独自のリガンド分類を行っている．検索された各 GPCR（またはリガンド）のページには，バイオ情報（またはケミカル情報），及びそれらに結合するリガンド（または GPCR）のリストが同時に表示される．さらに，GLIDA の GPCR（またはリガンド）のページは GPCR–リガンド相互作用の解析機能を有している．すなわち，検索された GPCR（またはリガンド）と最も高い類似性を持つ 25 個の GPCR（またはリガンド）リストを表示するとともに，これら 25 個のエントリーと結合するリガンド（または GPCR）との相互作用様式を 2 次元マップ表示する．このマップの 2 軸に並ぶ GPCR とリガンドの順番は，各々 GPCR とリガンドのクラスタリング結果を反映している．したがって，GPCR，リガンドの類似性情報と相互作用情報を同時に視覚化し，このパターンを分析して GPCR とリガンドの相互

作用予測を実現し，薬物と作用基点の相互作用に関する情報を得ることができる（Fig. 3, Fig. 4）．

5. ケミカルゲノミクスに基づくバーチャルスクリーニング

活性化合物を効率よく迅速に探し出すために，計算機を用いた候補化合物の絞り込み手法「バーチャルスクリーニング（VS）」が開発されてきた．現在よく用いられているVSとして，既知リガンドとの構造類似性に基づく「Ligand-based virtual screening（LBVS）」と標的タンパク質の立体構造に基づく「Structure-based virtual screening（SBVS）」がある．[5,6] この2つの手法は，近年の情報技術の進歩と相まって，この10–20年で著しい発展を遂げ，ゆるぎない地位を確立した．しかしながら現在，VSのヒット確率は1–10%もあればよしとされており（例えば，LBVSでは，既知活性化合物の骨格構造に強く影響される嫌いがあるし，SBVSでは，パラメータの恣意性，予測的中率の低さなどが指摘されている），さらなる技術的な改良や革新的技術の開発が切望されていることは間違いない．

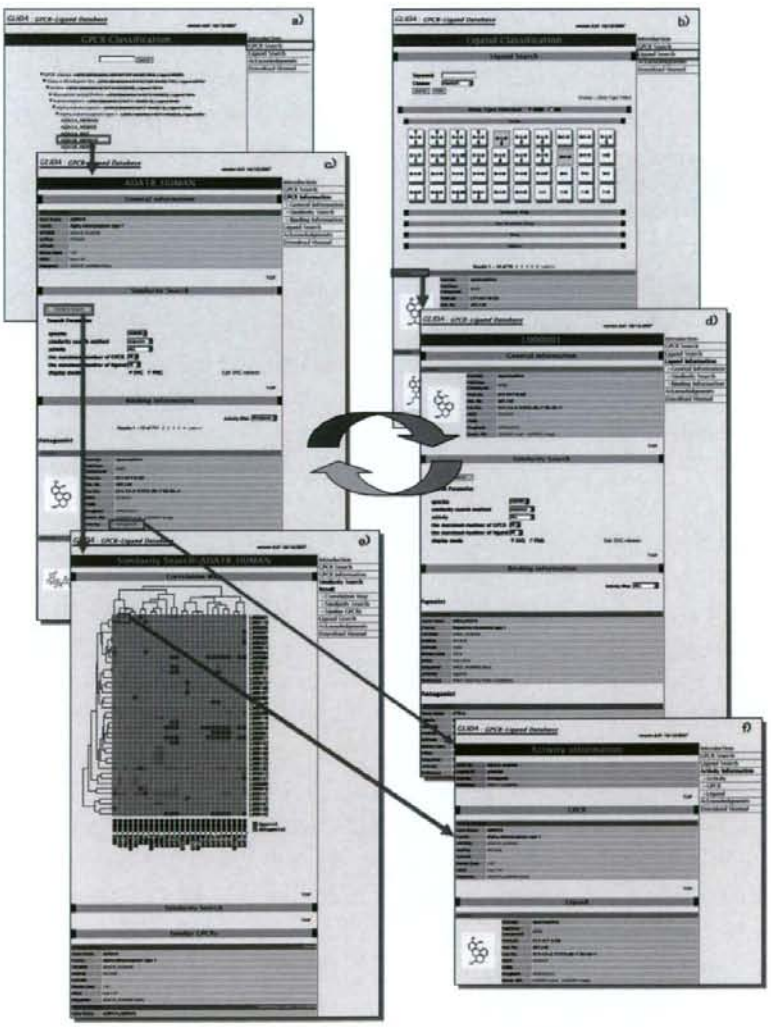

Fig. 3. A Screenshot of GLIDA Showing Linked Relations among Search Pages (a, b), Result Pages (c, d), an Analytical Report Page (e), and a Binding Information Page (f)

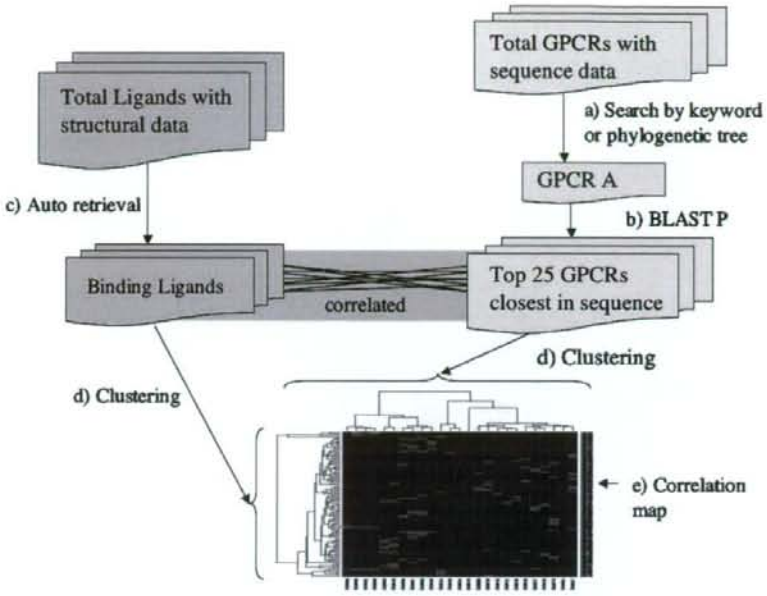

Fig. 4. A Schematic Example of the Search and Analysis Process Showing GPCR-ligand Correlations Produced from a GPCR Query Using GLIDA

ここでは，LBVS や SBVS とは概念の異なる第 3 の VS として，われわれが開発している「ケミカルゲノミクスに基づく VS 手法（Chemical Genomics-based virtual screening; CGBVS)」を紹介する．「ケミカルゲノミクス」は，興味を持つ化合物が生物に与える影響についてゲノム規模で研究する学問であり，[7,8] マイクロアレイやハイスループットスクリーニングなどの同時大量解析技術の革新に後押しされ，近年，注目を浴び始めている．それに伴い，化合物と遺伝子の関連性について，膨大な実験データが蓄積されている．そこでわれわれは，情報科学技術の 1 つであるパターン認識技術を用いて，タンパク質と化合物との結合情報（ケミカルゲノミクス情報）から抽出したタンパク質のリガンド認識パターンに基づいて活性化合物を効率的に発見する新たな VS，「CGBVS」を開発している．

タンパク質とリガンドとの相互作用パターンの認識とそのリガンド予測を開発するために，われわれは学習アルゴリズムの一種であるサポートベクターマシン（SVM)[9] を用いた．SVM は，2 クラス分類器の一種であり，与えられた 2 つのグループに属する特徴ベクトルを最大マージンで分離するような超平面を構築する．ここで，最大マージンとは，分離した超平面から各サンプル間までの最短距離を指す．

われわれは，この SVM を用いて，化合物–タンパク質相互作用の有／無を判別する手法を開発した．その手法の流れを Fig. 5 に示す．まず，収集した相互作用をベクトルとして表現するために，各化合物の化学構造，各タンパク質のアミノ酸配列について，様々な属性（記述子と呼ぶ）を計算する．次に，正例（相互作用する化合物–タンパク質ペア）及び負例（相互作用しない化合物–タンパク質ペア）に対応する記述子をそれぞれ組み合わせて特徴ベクトルを構成し，SVM を用いて学習モデルを構築する．このモデルが得られると，（未知の化合物–タンパク質ペアに相当する）新しいベクトルが相互作用有／無のどちらのクラスに属するかを予測することができる．

既存の VS 手法との比較検討を行うため，今回開発した CGBVS と LBVS との予測性能を比較した．収集した化合物–GPCR 相互作用を用いて，負例を交換しながら 5 分割交差検定法（5 fold cross-validation）を試行した．交差検定の結果，最近傍法を用いた LBVS では 84.4±0.3%，CGBVS では 91.6±0.2% の相互作用を正しく予測した．また，ROC 曲線からも，CGBVS の予測性能の高さが確

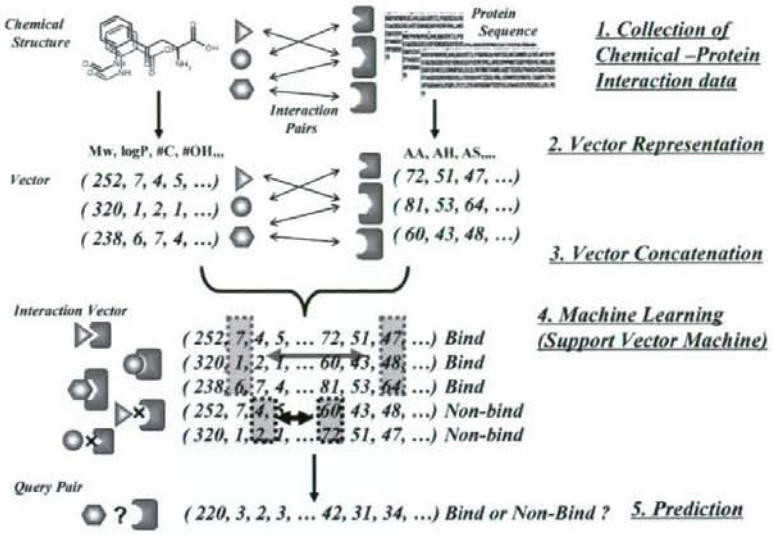

Fig. 5. Overview of Chemical Genomics-based Virtual Screening

認された（Fig. 6）．したがって，ケミカルゲノミクス情報の活用がリガンド予測性能の向上につながったといえる．

さらに，ヒト β2 アドレナリン受容体（β2AR）を標的 GPCR とし，構築した学習モデルを用いてリガンド予測を行い，*in vitro* 実験による検証を行った．リガンド予測の対象化合物は，β2AR 以外の GPCR のリガンドとして知られている 826 化合物とした．ここで，CGBVS により予測された β2AR リガンド候補上位 50 の化合物のうち，文献・特許調査により 14 種の化合物について β2AR との相互作用に関する報告を確認した．さらに，残りの相互作用不明な化合物のうち，入手可能な 21 種類について *in vitro* 結合阻害実験を行ったところ，17 種類の化合物が相互作用（10^{-5} M$<$IC$_{50}<10^{-3}$ M）を示した．結合阻害実験のヒット率は 81%（17/21）に上り，ここにおいても高い予測的中率が示された．また今回新たに発見した化合物の化学構造を精査したところ，典型的な β2AR 作動薬の構造（カテコラミン骨格，イソプレナリン誘導体）及び β2AR 拮抗薬の構造（アリルアルキルアミン誘導体）とは異なる多様な骨格を含んでおり，化合物の構造類似性に基づく従来の方法では発見が困難なリガンド群が含まれることが明らかになった．したがって，ケミカルゲノミクス情報が，リガンド予測精度の向上

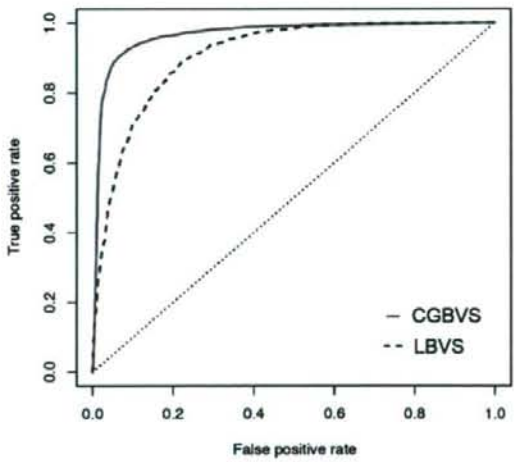

Fig. 6. Comparison of Prediction Performance between Chemical Genomics-based and Ligand-based Virtual Screenings

のみならず，新規骨格を持つリガンドの検出にも有用であることが示唆された．

6. おわりに

従来，生物活性を示す化合物の探索には，化合物の構造類似性がその指標とされてきた．しかし，化合物の構造類似性だけでタンパク質との多種多様な相互作用を見い出すには限界があり，新しい探索手法の開発が望まれていた．われわれは，「ケミカル

ゲノミクス情報の中から相互作用パターンを抽出する」という新しいアプローチを試み，1）化合物-GPCR 質間相互作用データベース GLIDA を開発し，2）学習アルゴリズムを用いた予測モデルにより，GPCR リガンドを精度よく予測できることを実証した．

なお，β2AR の立体構造が 2007 年決定された[10]ことを受けて，われわれは SBVS との予測性能比較も行っており，その結果，CGBVS が SBVS よりも高精度で β2AR リガンドを予測できることを確認している．

われわれが開発している CGBVS は，標的タンパク質のリガンド情報がないケースにも適用可能であり，実際に現在，オーファン GPCR を標的としたリガンド予測を行っている．タンパク質の立体構造情報を必要としない点は，詳細な 3D 構造が不明な GPCR にとって，魅力的なリガンド予測手法といえる．将来的には，結合阻害定数（Ki 値）など定量的な活性データから回帰分析を行うことにより，相互作用の強さを反映させたリガンド予測手法への拡張を行う予定である．ケミカルゲノミクス情報を利用するという新規なアプローチは，GPCR に限らずすべてのタンパク質に適用可能であり，化合物-タンパク質相互作用の理解，ひいては創薬プロセスの効率化につながることが期待される．

謝辞 本研究の一部は，文部科学省，経済産業省（NEDO 若手グラント），厚生労働省の助成金支援によって行われており，深く感謝申し上げる．本総説は，平成 20 年度日本薬学会奨励賞の受賞を記念して記述したものであり，日本薬学会役員，審査員の先生方をはじめご関係の皆様に心より感謝申し上げる．また，これまでご指導，ご鞭撻賜りました学生時代の恩師・杉浦幸雄先生（現同志社女子大学教授），研究員時代の恩師・金久 實先生（京都大学化学研究所教授），助手時代の恩師・辻本豪三先生（京都大学薬学研究科教授），並びに京都大学薬学研究科研究科長・藤井信孝先生に謹んで感謝の意を表します．

REFERENCES

1) *Nature*, **432** (7019) (Insight), 823–865 (2004).
2) Okuno Y., Yang J., Taneishi K., Yabuuchi H., Tsujimoto G., *Nucleic Acids Res.*, **34**, D673–677 (2006).
3) Okuno Y., Tamon A., Yabuuchi H., Niijima S., Minowa Y., Tonomura K., Kunimoto R., Feng C., *Nucleic Acids Res.*, **36**, D907–D912 (2008).
4) 〈http://pharminfo.pharm.kyoto-u.ac.jp/services/glida/〉
5) Muegge I., Oloff S., *Drug Discov. Today Technol.*, **3**, 405–411 (2006).
6) Oprea T. I., Matter H., *Curr. Opin. Chem. Biol.*, **8**, 49–58 (2004).
7) MacBeath G., *Genome Biol.*, **2**, COMMENT2005 (2001).
8) Salemme F. R., *Pharmacogenomics.*, **3**, 257–267 (2003).
9) Vapnik V. N., "The Nature of Statistical Learning Theory," Springer, New York, 1995.
10) Cerezov V., *Science.*, **318**, 1258–1265 (2007).

構造活性相関部会・ニュースレター <1 April, 2008>

SAR News No.14

「目次」

///// Perspective/Retrospective /////

ケミカルゲノミクス情報を用いた新規リガンド探索手法

京都大学薬学研究科　藪内　弘昭、奥野　恭史

1. はじめに

生体内には様々な分子が存在しているが、タンパク質は特定の分子を認識してその機能を発揮する。基礎生命科学から医薬品開発にわたる多くの分野では、この分子認識機構を利用して目的のタンパク質に結合して機能を制御するリガンド化合物の開発が長年進められてきた。しかし、化合物の化学構造は非常に多様性に富んでいる（10^{60}種類以上と推定されている[1]）ため、片っ端から合成、生物実験を行うことにも限界がある。

活性化合物を効率よく迅速に探し出すために、計算機を用いた候補化合物の絞り込み手法「ヴァーチャル・スクリーニング（VS）」が開発されてきた。現在よく用いられているVSとして、既知リガンドとの構造類似性に基づく「Ligand-based virtual screening（LBVS）」と標的タンパク質の立体構造に基づく「Structure-based virtual screening（SBVS）」がある[2,3]。この二つの手法は、近年の情報技術の進歩と相まって、この10-20年で著しい発展を遂げ、ゆるぎない地位を確立した。しかしながら現在、VSのヒット確率は1％－10%もあれば良しとされており（例えば、LBVSでは、既知活性化合物の骨格構造に強く影響される嫌いがあるし、SBVSでは、パラメータの恣意性、予測的中率の低さなどが指摘されている）、さらなる技術的な改良や革新的技術の開発が切望されていることは間違いない。

ここでは、LBVSやSBVSとは概念の異なる第三のVSとして、著者らが開発している「ケミカルゲノミクスに基づくVS手法（Chemical Genomics-based virtual screening: CGBVS）」を紹介したい。

2. ケミカルゲノミクス

「ケミカルゲノミクス（Chemical Genomics）」とは、興味を持つ化合物が生物に与える影響についてゲノム規模で研究する学問である[4,5]。この研究分野は、マイクロアレイやハイスループットスクリーニングなどの同時大量解析技術の革新に後押しされ、近年、注目を浴び始めている。それに伴い、化合物と遺伝子の関連性について、膨大な実験データが蓄積されている。そこで我々は、情報科学技術の一つであるパターン認識技術を用いて、タンパク質と化合物との結合情報（ケミカルゲノミクス情報）から抽出したタンパク質のリガンド認識パターンに基づいて活性化合物を効率的に発見する新たなVS、「CGBVS」を開発している。

3. ケミカルゲノミクス情報の収集・整備

CGBVSを実行するには、多くの「化合物-タンパク質間相互作用データ」が必要である。しかし残念ながら、それらのデータは基本的に製薬企業や各研究室の極秘資料となっている。そこで、我々はまず、文献などから利用可能な化合物-タンパク質相互作用データを収集、整備することからスタートした。データ収集の対象とするタンパク質としては、創薬標的として最も注目されている遺伝子ファミリーのひとつ、Gタンパク質共役型受容体（GPCR）に的を絞った。

収集したデータは、公共データベースGLIDA（GPCR-LIgand DAtabase）[6,7]として現在WEBで公開している（ URL: http://pharminfo.pharm.kyoto-u.ac.jp/services/glida/ ）。GLIDAの面白い特徴は、相互作用データを可視化するために、化合物、タンパク質それぞれの類似性を反映させた2次元カラーマップを用いている点である。マッピングされた相互作用において近傍に位置するタンパク質や化合物は、化学者にとっても生物学者にとっても、新たな研究対象として興味深いところである。